Lattice Dynamics Coupled to Charge and Spin Degrees of Freedom in the Molecular Dimer-Mott Insulator κ-$(BEDT\text{-}TTF)_2Cu[N(CN)_2]Cl$

Masato Matsuura,[1,*] Takahiko Sasaki,[2] Satoshi Iguchi,[2] Elena Gati,[3] Jens Müller,[3] Oliver Stockert,[4] Andrea Piovano,[5] Martin Böhm,[5] Jitae T. Park,[6] Sananda Biswas,[7] Stephen M. Winter,[7] Roser Valentí,[7] Akiko Nakao,[1] and Michael Lang[3]

[1]*Neutron Science and Technology Center, Comprehensive Research Organization for Science and Society (CROSS), Tokai, Ibaraki 319-1106, Japan*

[2]*Institute for Materials Research, Tohoku University, Sendai 980-8577, Japan*

[3]*Institute of Physics, Goethe-University Frankfurt, 60438 Frankfurt (M), Germany*

[4]*Max-Planck-Institut für Chemische Physik fester Stoffe, D-01187 Dresden, Germany*

[5]*Institut Laue-Langevin, 71 avenue des Martyrs, 38042 Grenoble Cedex 9, France*

[6]*Heinz Maier-Leibnitz Zentrum (MLZ), Technische Universität München, Lichtenbergstr. 1, 85748 Garching, Germany*

[7]*Institute for Theoretical Physics, Goethe-University Frankfurt, 60438 Frankfurt (M), Germany*

(Received 28 December 2018; revised manuscript received 24 May 2019; published 10 July 2019)

Inelastic neutron scattering measurements on the molecular dimer-Mott insulator κ-$(BEDT\text{-}TTF)_2Cu[N(CN)_2]Cl$ reveal a phonon anomaly in a wide temperature range. Starting from $T_{ins} \sim 50$–60 K where the charge gap opens, the low-lying optical phonon modes become overdamped upon cooling towards the antiferromagnetic ordering temperature $T_N = 27$ K, where also a ferroelectric ordering at $T_{FE} \approx T_N$ occurs. Conversely, the phonon damping becomes small again when spins and charges are ordered below T_N, while no change of the lattice symmetry is observed across T_N in neutron diffraction measurements. We assign the phonon anomalies to structural fluctuations coupled to charge and spin degrees of freedom in the BEDT-TTF molecules.

DOI: 10.1103/PhysRevLett.123.027601

Electronic ferroelectricity, where electrons and their interactions play the key role, has been in the focus of recent scientific efforts [1–3]. Whereas conventional ferroelectricity is driven by shifts in the atomic positions, electronic ferroelectricity originates from electronic degrees of freedom (d.o.f.), such as spin and charge, which offers an alternative route to control the system's ferroelectric properties. Electronic ferroelectricity, driven by spin d.o.f., is often found in frustrated magnetic systems with noncollinear spin structures [3,4]. In the case of the charge-driven variant, the electric dipoles arise from charge order or charge disproportionation in combination with dimerization, which has been found in inorganic oxides [5] and organic charge-transfer salts [6–10].

The κ-$(BEDT\text{-}TTF)_2X$ family, where BEDT-TTF is bis-(ethylenedithio)tetrathiafulvalene $C_6S_8[(CH_2)_2]_2$, is known to comprise bandwidth-controlled dimer-Mott systems where pairs of strongly interacting BEDT-TTF (in short ET) molecules form the dimers. In the dimer-Mott insulator picture, one π-hole carrier with spin $S = 1/2$ is localized on a molecular dimer unit. The charge d.o.f. may become active when this localization is no longer symmetric with respect to the center of the dimer but rather adopts an asymmetric state characterized by a charge disproportionation within the dimer [11,12]. Such a charge disproportionation scenario was suggested as the origin of the relaxor-type dielectric anomaly observed in the quantum-spin-liquid-candidate material $X = Cu_2(CN)_3$ (κ-CN) [8,13]—a suggestion that has created enormous attention as it highlights the important role of the intra-dimer charge d.o.f. Since relaxor ferroelectrics are known to consist of nanometer-sized domains, the relaxor-like dielectric anomaly in κ-CN suggests the presence of an inhomogeneous charge disproportionation. Recently, Lunkenheimer *et al.* have reported clear ferroelectric signatures in the related dimer-Mott system $X = Cu[N(CN)_2]Cl$ (κ-Cl) around the antiferromagnetic ordering temperature $T_N = 27$ K [14,15]. As in this system, long-range ferroelectricity of the order-disorder type is observed at $T_{FE} \approx T_N$, κ-Cl represents an ideal system to study the coupling of the charge to the spin and lattice d.o.f. in a dimer-Mott insulator.

It is fair to say that the origin of the electric dipoles in these dimer-Mott insulators is still under debate. Whereas for κ-Cl and κ-CN a definite proof of charge disproportionation is still missing [16], clear evidence for charge order within the ET dimers has recently been found for the more weakly dimerized compound $X = Hg(SCN)_2Cl$ [17], making this system a prime candidate for electronically driven ferroelectricity within the κ-$(ET)_2X$ family [10].

Given that there is a finite electron-lattice coupling, fluctuations of the electric dipoles are expected to give rise to anomalies in the lattice dynamics that can be sensitively probed by neutron scattering. In fact, for relaxor ferroelectrics, neutron scattering studies have been able to reveal

a phonon anomaly upon the appearance of inhomogeneous and fluctuating polar domains [18].

Unfortunately, systematic inelastic neutron scattering (INS) studies on organic charge-transfer salts have often been hampered due to the lack of sufficiently large single crystals with only a few exceptions: for instance, a sizable phonon renormalization effect on entering the superconducting state was reported for the organic superconductor κ-$(ET)_2Cu(NCS)_2$ [19]. Thanks to major recent improvements in focusing the neutron beam, however, the situation has improved considerably. As we demonstrate in this work, the largely enhanced neutron flux at the sample position in state-of-the-art triple-axis spectrometers [20,21] now enables such INS studies to be performed even on small single crystals of organic charge-transfer salts. Here we report an INS study of the lattice dynamics and its coupling to the charge and spin d.o.f. for the dimer-Mott insulator κ-Cl. By using an array of co-aligned single crystals of deuterated κ-Cl with total mass of 7 and 9 mg, we were able to detect clear phonon signals the amplitude of which shows a striking variation upon changing the temperature. We found that the low-lying optical phonon modes at 2.6 meV become damped below the onset temperature of the dimer-Mott insulating state in which the π carriers start to localize on the dimer sites. This phonon damping becomes small again on cooling below T_N. In contrast to conventional displacive ferroelectrics, however, there is no divergence of the phonon intensity nor any change in the lattice symmetry at T_N, where also the dielectric anomaly was observed. Thus, in κ-Cl the lattice is clearly coupled to the charge and spin d.o.f. but appears not to be the driving force of the antiferromagnetic-ferroelectric phase transition at T_N/T_{FE}.

Deuterated single crystals of κ-$(ET)_2Cu[N(CN)_2]Cl$ were grown by electrochemical crystallization. The Néel temperature was determined to be $T_N = 27$ K from magnetic susceptibility measurements as shown in Fig. 3(d), which is identical to the ordering temperature reported for hydrogenated κ-Cl [22]. INS experiments were performed on the triple-axis spectrometers IN8 at the Institut Laue-Langevin [20] and PUMA at the Heinz Maier-Leibnitz Zentrum [21]. All data were collected with a fixed final neutron energy of 14.7 meV using a doubly focused Cu analyzer for IN8 and a doubly focused pyrolytic graphite (PG) analyzer for PUMA. The initial neutron energy was selected by a doubly focused PG monochromator for both IN8 and PUMA. A PG filter was placed in front of the analyzer to suppress the scattering of higher-order neutrons. To improve the signal-to-noise ratio, two single crystals with a total mass of 7 mg, and six single crystals with a total mass of 9 mg were co-aligned for the neutron experiments on IN8 and PUMA, respectively. In all experiments, the samples were slowly cooled with 1 K/min around $T = 75$ K to minimize disorder in the ET molecules' ethylene end group orientations [23,24]. The single crystals were mounted so as to access the $(h0l)$ and $(hk0)$ scattering plane for INS and neutron diffraction measurements, respectively. Throughout this Letter, we label the momentum transfer in units of the reciprocal lattice vectors $a^* = 0.484$, $b^* = 0.210$, and $c^* = 0.741$ Å^{-1}. The instrumental energy resolution for IN8 linearly increases from 0.45 ($E = 0$) to 0.84 meV ($E = 10$ meV). To relate the fit parameters to the scattering function of the sample, convolution of the instrumental resolution at $E = 3$ meV has been included and computed using the RESTRAX simulation package [25]. We assume flat dispersions within Q width of the resolution ellipsoid since optical dispersions close to the Γ point are flat.

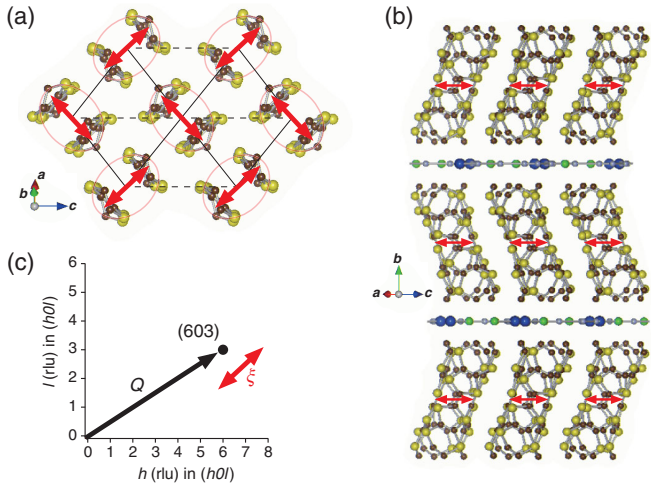

FIG. 1. Crystal structure of κ-$(ET)_2Cu[N(CN)_2]Cl$: (a) Top view of the ET layer and (b) side view of the layered structure. (c) Wave vector $\boldsymbol{Q} = (603)$ chosen for phonon measurements in the $(h0l)$ scattering plane. Ellipses in (a) indicate ET dimers. Thick arrows show schematically the breathing mode with polarization vector $\boldsymbol{\xi}$ of ET molecules mainly detected at (603).

Figures 1(a) and 1(b) show the crystal structure of κ-Cl consisting of layers of ET molecules separated by thin anion sheets. The ET molecules form dimers, resulting in a dimer-Mott insulating ground state. Since the distance between the ET molecules within the dimer reflects the degree of dimerization, some of the modes are expected to couple more strongly to the electronic d.o.f. than others. One such mode is a breathing mode of the ET dimers, shown schematically by thick arrows in Figs. 1(a) and 1(b). The scattering intensity of phonons in neutron scattering is proportional to $(\boldsymbol{Q} \cdot \boldsymbol{\xi})^2$, where $\boldsymbol{Q}$ is the momentum transfer between the initial and final state of the neutron, and ξ is the polarization vector of the phonon mode. Thus, the breathing of the ET dimers can best be measured when $\boldsymbol{Q}$ is large and parallel to ξ of the breathing mode as shown in Fig. 1(c). We measured the phonon spectra mainly at (603) to detect changes in the low-lying vibrational modes which are likely coupled to the charge and spin d.o.f.; changes will be detected for any vibrational mode which has a component parallel to [603].

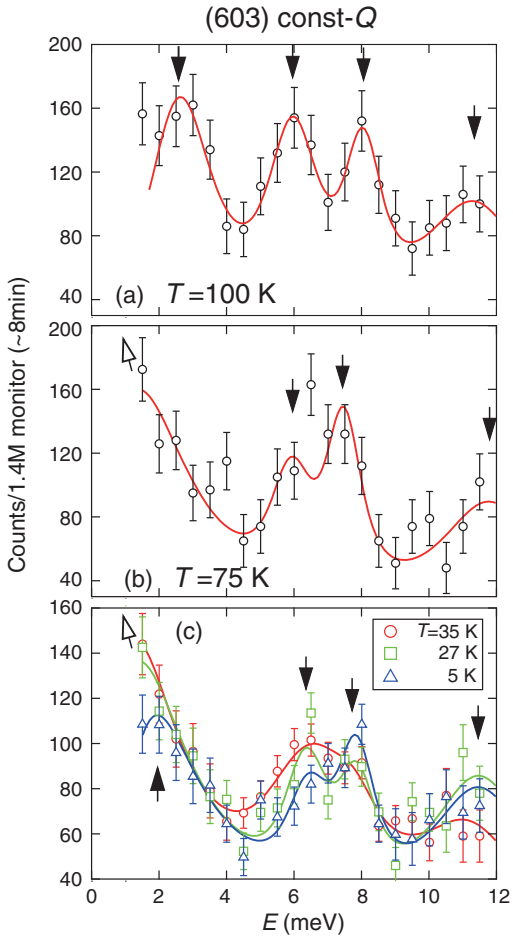

FIG. 2. Temperature dependences of constant-Q scans at (603) measured by using IN8. The solid lines are fits to four damped harmonic oscillator functions at $E \sim 2.6$, 6, 8, and 11 meV. The instrumental resolution was convolved to the model cross sections assuming flat dispersion within the resolution. Closed arrows indicate underdamped phonon modes, while open arrows show the overdamped phonon mode for $T_N < T \leq 75$ K.

Figures 2(a)–2(c) show constant-Q scans at (603) measured at various temperatures. At $T = 100$ K, we observe clear phonon peaks at $E = 2.6$, 6, 8, and 11 meV shown by the closed arrows. (See Figs. S1 and S2 in the Supplemental Material for the details of the dispersion [26]). The peak width for the low-lying modes at $E = 2.6$ meV (full width at half maximum; 2.3 meV) is considerably larger than the energy resolution (0.5 meV) indicating a finite lifetime due to phonon-phonon or electron-phonon interactions. For an anharmonic phonon, the energy dependence of the scattering function can be expressed by the damped harmonic-oscillator function [29]

$$\frac{\Gamma_q \hbar\omega}{[\hbar^2(\omega^2 - \omega_q^2)]^2 + (\Gamma_q \hbar\omega)^2}, \tag{1}$$

where $\hbar\omega$ is the energy transfer between the initial and final state of the neutron, and Γ_q denotes the damping factor. The lifetime of the phonons is inversely proportional to Γ_q. The enhanced phonon width, when compared to the energy resolution, suggests a strongly anharmonic lattice, consistent with the observation of large expansion coefficients in the κ-$(ET)_2X$ family [23]. On cooling, the well-resolved peak from the low-lying optical modes at 2.6 meV changes into a sloped signal at $T = 75$ K, whereas the three modes at 6, 8, and 11 meV remain at almost the same energy [Fig. 2(b)]. When the damping factor Γ_q becomes comparable to ω_q, the phonon spectrum changes into a single peak at $E = 0$. The sloped spectrum can be explained by an increasing Γ_q for the low-lying optical modes, which indicates the short lifetime of these modes. Similar phonon spectra at low energies are observed down to $T_N = 27$ K [Fig. 2(c)]. Below T_N, the truly inelastic nature of the low-lying optical modes become again visible.

Figure 3(a) shows the temperature dependence of the damping factor Γ_q for the low-lying optical modes. Note that Γ_q is comparable to ω_q in a wide temperature range for $T_N < T < 75$ K, indicating the damped nature of the low-lying optical modes. In addition to the phonon anomaly, we find that the energy width of the Bragg peaks is broadened in the same temperature range (Fig. S3 in the Supplemental Material [26]), suggesting an unstable lattice in this temperature region. Thus, the lattice of κ-Cl shows anomalous behavior in a wide temperature range above T_N.

Overdamped soft modes are often seen near structural phase transitions in a variety of materials. In the overdamped regime, the scattering function $S(\boldsymbol{Q}, \omega)$ is approximated as [30]:

$$S(\boldsymbol{Q}, \omega) = \frac{(2\pi)^3}{v_0} |F(\boldsymbol{Q})|^2 \frac{k_B T}{\hbar\omega_q^2} \frac{1}{\pi} \frac{\gamma_q}{\omega^2 + \gamma_q^2}, \tag{2}$$

where v_0 is the unit cell volume, $F(\boldsymbol{Q})$ is a dynamical structure factor, and $\gamma_q = [(\omega_q^2)/(2\Gamma_q)]$. Thus, the integrated intensity of an overdamped soft mode [$I_{\text{damp}} = \int S(\boldsymbol{Q},\omega) d\omega$] is proportional to $k_B T/\omega_q^2$. As $\omega_{q=0}$ goes to zero at the transition temperature, the intensity of the damped soft mode diverges and T/I_{damp} goes to zero. Figure 3(b) shows the temperature dependence of T/I_{damp} for the low-lying optical modes. Clearly, T/I_{damp} does not vanish at T_N, which indicates that the structural change is not the primary order parameter for the phase transition at T_N. This is consistent with the observation of only a small anomaly in the thermal expansion at $T_N \approx T_{FE}$ for κ-Cl [23]. Instead, other d.o.f. show divergent behavior at T_N, namely $(T_1 T)^{-1}$ of ^1H NMR for the spin [22] and the dielectric constant for the charge d.o.f. [14].

Note that the overdamped phonon appears already at 60–75 K, which is much higher than T_N. Figure 3(c) shows the temperature dependence of the scattering intensity at $Q = (603)$ and $E = 1.5$ meV. The effect of the phonon anomaly is clearly seen as an enhancement of the intensity at low energies ($E = 1.5$ meV) for $T_N < T \lesssim 60$ K. The coupling between a phonon mode and a relaxation

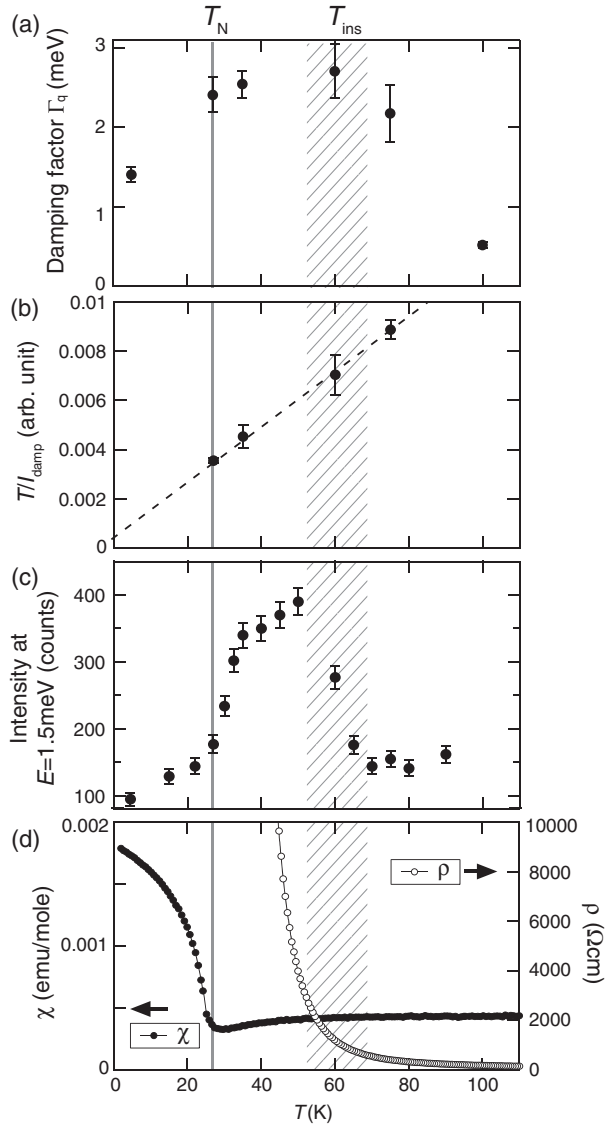

FIG. 3. Temperature dependence of (a) the damping factor Γ_q for the low-lying optical modes at (603), (b) T/I_{damp} for the low-lying optical modes (see text for details), (c) the intensity at $E = 1.5$ meV at (603), (d) the out-of-plane electrical resistivity ($\|b$) and out-of-plane dc magnetic susceptibility ($\|b$) at $\mu_0 H = 0.5$ T. The hatched area at ~50–60 K represents the crossover temperature T_{ins} as described in the text. The broken line in (b) is a linear fit. Data in (a) were measured at IN8 while data in (c) were obtained at PUMA.

mode of different origin (represented by a pseudospin) was discussed by Yamada within a pseudospin-phonon coupling model [31]. In this model, the relaxation mode and the phonon mode become strongly coupled when the characteristic frequency and wave vector of the pseudospin's relaxation mode roughly match those of the phonon mode, which results in a broadening of the phonon in energy. The structural fluctuations between the two ethylene end group orientations of the ET molecules, known to occur in the κ phase $(\mathrm{ET})_2X$ salts [24,32], however, cannot be the origin of the observed phonon anomaly since the ethylene end group motion freezes out in a glassy fashion below about 75 K.

On the other hand, the onset temperature of the phonon anomaly roughly coincides with the rapid increase in the electrical resistivity below $T_{\mathrm{ins}} \sim 50$–60 K, as shown in Fig. 3(d). Optical conductivity measurements have revealed that the charge gap starts to open below T_{ins} [33,34], indicating charge localization at the ET dimer site. Even after the itinerant π carriers become localized at the dimer site below T_{ins}, the distribution of charge within the dimer remains as an active d.o.f. The coincidence of the onset temperature of the phonon anomaly and T_{ins} suggests a coupling between the lattice and this intradimer charge d.o.f. A similar scenario was observed in the organic superconductor κ-$(\mathrm{ET})_2\mathrm{Cu(NCS)}_2$ for the lowest optical mode [19]. We thus expect that the low-lying optical modes are the key modes where the electron-phonon coupling becomes manifest in these organic salts containing ET molecules.

In an attempt to identify the low-lying optical modes with the theoretically obtained vibrational frequencies, we considered the phonon frequencies of the closely related system κ-CN [35], which has a similar arrangement of anion and ET layers as κ-Cl, but exhibits considerably less phonon modes. The calculated lowest optical mode in κ-CN at $q = 0$ has an energy of 3 meV and two of the ET-dimer breathing modes, involving also the movements of the anion layers, lie at energies of 4.1 and 4.7 meV. The κ-Cl system differs from κ-CN mainly in two ways: (i) the ET dimers in κ-Cl are alternately stacked along the b axis, thus doubling the unit cell along that direction and (ii) the anion layers consist of chains arranged in a polymeric zigzag pattern, instead of having a more rigid two-dimensional network in κ-CN. It is to be expected that these factors will lead to significantly softer spring constants in κ-Cl compared to κ-CN. Such a rescaling of the phonon modes would affect all the phonons in the low-frequency regime. The lowest mode in κ-CN may shift toward very low energies and merge with the elastic peak, which may allow us to identify the observed low-lying optical modes in κ-Cl as an ET-dimer breathing mode.

Below T_{N}, the damping of the low-lying optical modes become small as shown in Figs. 2(c) and 3(a). According to the pseudospin-coupling model [31], the reduction in the damping factor Γ_q is due to the decoupling between the lattice and the pseudospins as a consequence of a critical slowing down of the pseudospin fluctuations. Since both dielectric and antiferromagnetic fluctuations freeze out below T_{N} [14], the recovery of a truly inelastic phonon peak suggests a close correlation between lattice, spin, and charge d.o.f. at the phase transition at $T_{\mathrm{N}} \approx T_{\mathrm{FE}}$.

In order to check for the possibility of a change in the crystallographic symmetry at T_{N}, we performed detailed neutron diffraction measurements on a deuterated single crystal of κ-Cl at $T = 35$ K ($>T_{\mathrm{N}}$) and 4 K ($<T_{\mathrm{N}}$) (Fig. S4 in the Supplemental Material [26]). As explained in detail in the Ref. [26], we did not find any indications for

a crystallographic symmetry lowering at $T_N \approx T_{FE}$. This supports the picture of electronic ferroelectricity, where instead of the lattice, the spin or charge d.o.f. are the driving force of the phase transition in κ-Cl.

In discussing our results, we recall that recent vibrational spectroscopy studies failed to detect clear signatures of a charge disproportionation in κ-Cl and κ-CN [16]. On the other hand, our finding of overdamped modes for $T_N < T \lesssim T_{ins}$ strongly suggests a close coupling between the lattice and the intradimer charge d.o.f. According to the pseudospin-coupling model [31], the characteristic energy of the charge fluctuations is expected to be in the same range as the low-lying optical modes, 1–2 meV, for $T_N < T \lesssim T_{ins}$. This energy scale is 2 orders of magnitude smaller than that of the charge-sensitive mode studied in the above-mentioned vibrational spectroscopy experiments. Furthermore, a finite dc conductivity is observed even in the "Mott-insulating" state below $\sim T_{ins}$ reflecting some degree of remaining itinerancy of the fluctuating π electrons. The complex and seemingly contradictory picture of the low energy charge dynamics reported so far is likely due to the different timescales of the investigated characteristic mode.

To summarize, by studying the spectra of selected phonons of the dimer-Mott insulator κ-$(ET)_2Cu[N(CN)_2]Cl$ as a function of temperature, we found clear renormalization effects which can be associated with charge fluctuations. We argue that the overdamped optical phonon modes, observed in a wide temperature range from $T_{ins} \sim 50$–60 K down to $T_N \approx T_{FE}$, result from a coupling of the lattice to the intradimer charge d.o.f. We consider these inelastic neutron scattering results as an important step that may trigger further systematic studies on the lattice dynamics and its coupling to the electronic d.o.f. in the family of organic charge-transfer salts.

We are grateful to M. Naka and S. Ishihara for helpful discussions. We also thank O. Sobolev, M. Kurosu, R. Kobayashi, B. Hartmann, T. Ohhara, and K. Munakata for their help in the experiments. The neutron experiments were performed with the approval of ILL (7-01-401) [36], MLZ (11879), and J-PARC MLF (2017B0201). The crystal structures in Fig. 1 are produced by VESTA software [37]. This study was financially supported by Grants-in-Aid for Scientific Research (Grants No. 25287080, No. 19H01833, No. 16K05430, and No. 18H04298) from the Japan Society for the Promotion of Science and by the Deutsche Forschungsgemeinschaft (DFG) within the collaborative research center SFB/TR 49 "Condensed Matter Systems with Variable Many-Body Interactions."

*m_matsuura@cross.or.jp

[1] J. Van Den Brink and D. I. Khomskii, Multiferroicity due to charge ordering, J. Phys. Condens. Matter **20**, 434217 (2008).
[2] S. Horiuchi and Y. Tokura, Organic ferroelectrics, Nat. Mater. **7**, 357 (2008).
[3] S. Ishihara, Electronic ferroelectricity and frustration, J. Phys. Soc. Jpn. **79**, 011010 (2010).
[4] T. Kimura, T. Goto, H. Shintani, K. Ishizaka, T. h. Arima, and Y. Tokura, Magnetic control of ferroelectric polarization, Nature (London) **426**, 55 (2003).
[5] N. Ikeda, H. Ohsumi, K. Ohwada, K. Ishii, T. Inami, K. Kakurai, Y. Murakami, K. Yoshii, S. Mori, and Y. Horibe, Ferroelectricity from iron valence ordering in the charge-frustrated system $LuFe_2O_4$, Nature (London) **436**, 1136 (2005).
[6] D. S. Chow, F. Zamborszky, B. Alavi, D. J. Tantillo, A. Baur, C. A. Merlic, and S. E. Brown, Charge Ordering in the TMTTF Family of Molecular Conductors, Phys. Rev. Lett. **85**, 1698 (2000).
[7] K. Yamamoto, S. Iwai, S. Boyko, A. Kashiwazaki, F. Hiramatsu, C. Okabe, N. Nishi, and K. Yakushi, Strong Optical Nonlinearity and its Ultrafast Response Associated with Electron Ferroelectricity in an Organic Conductor, J. Phys. Soc. Jpn. **77**, 074709 (2008).
[8] M. Abdel-Jawad, I. Terasaki, T. Sasaki, N. Yoneyama, N. Kobayashi, Y. Uesu, and C. Hotta, Anomalous dielectric response in the dimer Mott insulator κ-$(BEDT\text{-}TTF)_2Cu_2(CN)_3$, Phys. Rev. B **82**, 125119 (2010).
[9] S. Iguchi, S. Sasaki, N. Yoneyama, H. Taniguchi, T. Nishizaki, and T. Sasaki, Relaxor ferroelectricity induced by electron correlations in a molecular dimer Mott insulator, Phys. Rev. B **87**, 075107 (2013).
[10] E. Gati, J. K. H. Fischer, P. Lunkenheimer, D. Zielke, S. Köhler, F. Kolb, H.-A. K. von Nidda, S. M. Winter, H. Schubert, J. A. Schlueter *et al.*, Evidence for Electronically Driven Ferroelectricity in a Strongly Correlated Dimerized BEDT-TTF Molecular Conductor, Phys. Rev. Lett. **120**, 247601 (2018).
[11] M. Naka and S. Ishihara, Electronic ferroelectricity in a dimer Mott insulator, J. Phys. Soc. Jpn. **79**, 063707 (2010).
[12] C. Hotta, Theories on frustrated electrons in two-dimensional organic solids, Crystals **2**, 1155 (2012).
[13] Y. Shimizu, K. Miyagawa, K. Kanoda, M. Maesato, and G. Saito, Spin Liquid State in an Organic Mott Insulator with a Triangular Lattice, Phys. Rev. Lett. **91**, 107001 (2003).
[14] P. Lunkenheimer, J. Müller, S. Krohns, F. Schrettle, A. Loidl, B. Hartmann, R. Rommel, M. de Souza, C. Hotta, and J. A. Schlueter, Multiferroicity in an organic charge-transfer salt that is suggestive of electric-dipole-driven magnetism, Nat. Mater. **11**, 755 (2012).
[15] M. Lang, P. Lunkenheimer, J. Müller, A. Loidl, B. Hartmann, N. H. Hoang, E. Gati, H. Schubert, and J. A. Schlueter, Multiferroicity in the Mott insulating charge-transfer salt $\kappa-(BEDT\text{-}TTF)_2Cu[N(CN)_2]Cl$, IEEE Trans. Magn. **50**, 2700107 (2014).
[16] K. Sedlmeier, S. Elsässer, D. Neubauer, R. Beyer, D. Wu, T. Ivek, S. Tomić, J. A. Schlueter, and M. Dressel, Absence of charge order in the dimerized κ-phase BEDT-TTF salts, Phys. Rev. B **86**, 245103 (2012).
[17] N. Drichko, R. Beyer, E. Rose, M. Dressel, J. A. Schlueter, S. A. Turunova, E. I. Zhilyaeva, and R. N. Lyubovskaya, Metallic state and charge-order metal-insulator transition in the quasi-two-dimensional conductor $\kappa-(BEDT\text{-}TTF)_2Hg(SCN)_2Cl$, Phys. Rev. B **89**, 075133 (2014).

[18] P. M. Gehring, S. E. Park, and G. Shirane, Soft Phonon Anomalies in the Relaxor Ferroelectric $Pb(Zn_{1/3}Nb_{2/3})_{0.92}Ti_{0.08}O_3$, Phys. Rev. Lett. **84**, 5216 (2000).

[19] L. Pintschovius, H. Rietschel, T. Sasaki, H. Mori, S. Tanaka, N. Toyota, M. Lang, and F. Steglich, Observation of superconductivity-induced phonon frequency changes in the organic superconductor $\kappa-(\mathrm{BEDT\text{-}TTF})_2\mathrm{Cu(NCS)}_2$, Europhys. Lett. **37**, 627 (1997).

[20] A. Hiess, M. Jiménez-Ruiz, P. Courtois, R. Currat, J. Kulda, and F. J. Bermejo, ILL's renewed thermal three-axis spectrometer IN8: A review of its first three years on duty, Physica (Amsterdam) **385B**, 1077 (2006).

[21] H. M.-L. Zentrum, PUMA: Thermal three axes spectrometer, J. Large-Scale Res. Facil. **1**, A13 (2015).

[22] K. Miyagawa, A. Kawamoto, Y. Nakazawa, and K. Kanoda, Antiferromagnetic Ordering and Spin Structure in the Organic Conductor, $\kappa-(\mathrm{BEDT\text{-}TTF})_2\mathrm{Cu[N(CN)}_2]\mathrm{Cl}$, Phys. Rev. Lett. **75**, 1174 (1995).

[23] J. Müller, M. Lang, F. Steglich, J. A. Schlueter, A. M. Kini, and T. Sasaki, Evidence for structural and electronic instabilities at intermediate temperatures in $\kappa-(\mathrm{BEDT\text{-}TTF})_2X$ for $X=\mathrm{Cu[N(CN)}_2]\mathrm{Cl}$,$\mathrm{Cu[N(CN)}_2]\mathrm{Br}$ and $\mathrm{Cu(NCS)}_2$: Implications for the phase diagram of these quasi-two-dimensional organic superconductors, Phys. Rev. B **65**, 144521 (2002).

[24] J. Müller, B. Hartmann, R. Rommel, J. Brandenburg, S. M. Winter, and J. A. Schlueter, Origin of the glass-like dynamics in molecular metals $\kappa-(\mathrm{BEDT\text{-}TTF})_2\mathrm{X}$: implications from fluctuation spectroscopy and ab initio calculations, New J. Phys. **17**, 083057 (2015).

[25] J. Saroun and J. Kulda, RESTRAX - a program for TAS resolution calculation and scan profile simulation, Physica (Amsterdam) **234B**, 1102 (1997).

[26] See Supplemental Material at http://link.aps.org/supplemental/10.1103/PhysRevLett.123.027601 for the details of the dispersion, the energy width of the Bragg peak, and the neutron diffraction measurements, which includes Refs. [27,28].

[27] T. Ohhara, R. Kiyanagi, K. Oikawa, K. Kaneko, T. Kawasaki, I. Tamura, A. Nakao, T. Hanashima, K. Munakata, T. Moyoshi *et al.*, SENJU: a new time-of-flight single-crystal neutron diffractometer at J-PARC, J. Appl. Crystallogr. **49**, 120 (2015).

[28] J. M. Williams, A. M. Kini, H. H. Wang, K. D. Carlson, U. Geiser, L. K. Montgomery, G. J. Pyrka, D. M. Watkins, J. M. Kommers, and S. J. Boryschuk, From semiconductor-semiconductor transition (42 K) to the highest-Tc organic superconductor, $\kappa-(\mathrm{ET})_2\mathrm{Cu[N(CN)}_2]\mathrm{Cl}$ ($T_c = 12.5$ K), Inorg. Chem. **29**, 3272 (1990).

[29] K. Gesi, J. D. Axe, G. Shirane, and A. Linz, Dispersion and damping of soft zone-boundary phonons in $KMnF_3$, Phys. Rev. B **5**, 1933 (1972).

[30] G. Shirane, S. M. Shapiro, and J. M. Tranquada, *Neutron Scattering with a Triple-Axis Spectrometer: Basic Techniques* (Cambridge University Press, Cambridge, England, 2002).

[31] Y. Yamada, H. Takatera, and D. L. Huber, Critical dynamical phenomena in pseudospin-phonon coupled systems, J. Phys. Soc. Jpn. **36**, 641 (1974).

[32] U. Geiser, A. J. Schults, H. H. Wang, D. M. Watkins, D. L. Stupka, J. M. Williams, J. E. Schirber, D. L. Overmyer, D. Jung, and J. J. Novoa, Strain index, lattice softness and superconductivity of organic donor-molecule salts: Crystal and electronic structures of three isostructural salts $\kappa-(\mathrm{BEDT\text{-}TTF})_2\mathrm{Cu[N(CN)}_2]\mathrm{X}$ ($\mathrm{X}=\mathrm{Cl, Br, I}$), Physica (Amsterdam) **174C**, 475 (1991).

[33] K. Kornelsen, J. E. Eldridge, H. H. Wang, H. A. Charlier, and J. M. Williams, Infrared study of the metal-insulator transition in the organic conductor $\kappa-(\mathrm{BEDT\text{-}TTF})_2\mathrm{Cu[N(CN)}_2]\mathrm{Cl}$, Solid State Commun. **81**, 343 (1992).

[34] T. Sasaki, I. Ito, N. Yoneyama, N. Kobayashi, N. Hanasaki, H. Tajima, T. Ito, and Y. Iwasa, Electronic correlation in the infrared optical properties of the quasi-two-dimensional κ-type BEDT-TTF dimer system, Phys. Rev. B **69**, 064508 (2004).

[35] M. Dressel, P. Lazić, A. Pustogow, E. Zhukova, B. Gorshunov, J. A. Schlueter, O. Milat, B. Gumhalter, and S. Tomić, Lattice vibrations of the charge-transfer salt $\kappa-(\mathrm{BEDT\text{-}TTF})_2\mathrm{Cu}_2(\mathrm{CN})_3$: Comprehensive explanation of the electrodynamic response in a spin-liquid compound, Phys. Rev. B **93**, 081201(R) (2016).

[36] M. Matsuura, M. Lang, J. Müller, T. Sasaki, O. Stockert, and A. Wildes, Study of multiple coupling between the spin, charge, and lattice in a multiferroic organic charge-transfer salt $\kappa-(\mathrm{BEDT\text{-}TTF})_2\mathrm{Cu[N(CN)}_2]\mathrm{Cl}$ (Institut Laue-Langevin (ILL), Grenoble, 2014), https://doi.ill.fr/10.5291/ILL-DATA.7-01-401.

[37] K. Momma and F. Izumi, VESTA 3 for three-dimensional visualization of crystal, volumetric and morphology data, J. Appl. Crystallogr. **44**, 1272 (2011).